Electromagnetic Band Gap Structures: Practical Tips and Advice for Antenna Engineers

Peter KOVÁCS, Tomáš URBANEC

Dept. of Radio Electronics, Brno University of Technology, Purkyňova 118, 612 00, Brno, Czech Republic

kovacsp@feec.vutbr.cz, urbanec@feec.vutbr.cz

Abstract. *In this paper we discuss the use of electromagnetic band gap (EBG) structures in antenna engineering from a practical point of view. Our aim is to point out the most common mistakes and myths related to design, analysis and application of EBGs in the field of antennas. The paper could be helpful for beginners giving a short course on designing EBGs but also will bring novel findings for experts, investigating the effect of different number of unit cells on radiation characteristics of a planar antenna. An important part of the paper is the experiments showing the surface wave distribution over an EBG board and over the fabricated antennas with and without the periodic structure.*

Keywords

Electromagnetic band gap (EBG), surface wave distribution, patch antenna, radiation properties.

1. Introduction

The major problem associated with planar antennas originates in the guiding of plane waves by a plane interface between two different media: conductor-dielectrics or dielectrics-dielectrics. The electromagnetic energy trapped between the interfaces, and forming into surface waves, is substantial: an elementary dipole, placed on a uniform substrate with no losses and represented by the relative dielectric constant ε, radiates $\varepsilon^{3/2}$ times more power into the substrate than into the air; a second problem is that the electromagnetic waves radiated into substrate and reaching the dielectric-air interface at angles greater than $\theta_c = \sin^{-1} \varepsilon^{-1/2}$ are totally reflected [1], [2]. The power transferred into the surface waves does not contribute to the main radiation of the antenna, but it is scattered off the edges of the finite ground plane and leads to deep nulls and ripples in radiation patterns, increased back radiation, gain deterioration, lower polarization purity, etc. In general, the higher the permittivity of dielectrics and thicker the substrate, the stronger the influence of the surface waves.

During last decades, many techniques were developed to reduce surface waves excited by printed antennas. To name only a few: drilling an air cavity below the patch [3], placing an additional dielectric layer over the patch [4] or optimizing the patch shape so that the surface waves are not excited [5]. In the late 80's, a novel structure called *photonic band gap* (PBG) has been introduced. The structure was able to permit electromagnetic wave propagation in certain frequency bands called *band gaps* [6], [7]. After successful implementation of PBGs in photonics, they became widely used also in microwave and antenna engineering as *electromagnetic band gap* (EBG) surfaces [8]. EBGs make possible to intensively suppress surface waves in printed antenna boards. The most widely used type of EBGs are metallo-dielectric structures, consisting of periodic array of patches, connected (mushroom type) or not (planar type) to the ground plane (Fig. 1). The mushroom and planar EBG differs in many aspects and which to choose always depends on application. For successful implementation in practice, also particular care should be paid to their correct design and computer modeling.

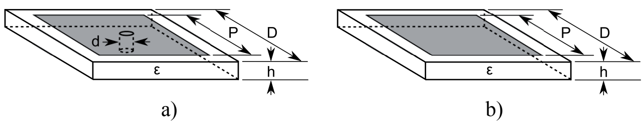

Fig. 1. Mushroom (a) and planar (b) metallo-dielectric EBG. The parameters are: period *D*, size of the square patch *P*, via diameter *d*, dielectric slab thickness *h* and dielectric slab permittivity *ε*.

The main goal of this paper is to clarify some common mistakes related to use of electromagnetic band gap structures in antenna engineering and to give the reader a brief and clear overview about their basic theory and numerical simulations. On the other hand, we also demonstrate the practical exploitation of EBGs on measurement examples. The most original contribution of the paper is the investigation of different number of EBG unit cells on performance of a probe-fed planar antenna. The presented experiments could be useful for designers to achieve the desired radiation characteristics of a planar antenna and to keep its size as small as possible.

2. Theory

2.1 Mushroom or Planar EBG?

Let us investigate the prerequisites for transverse magnetic (TM) and transverse electric (TE) surface wave propagation on a general impedance surface whose properties can be described with a single parameter, the surface impedance Z_s [1], [8]. The surface is positioned in the *y-z* plane as shown in Fig. 2. A surface wave propagates in the +*z* direction with the fields decaying exponentially with decay constant α in the +*x* direction.

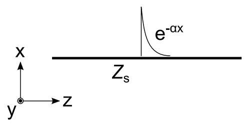

Fig. 2. A surface wave on an impedance surface.

For TM surface waves, the *x* and *z* components of the magnetic field intensity and the *y* component of the electric field intensity are equal to zero, $H_x = H_z = E_y = 0$. The surface wave impedance can be expressed as the ratio of the electric field over the magnetic field at the surface [1], [8]

$$Z_s(TM) = \frac{E_z}{H_y} = \frac{j \cdot \alpha}{\omega \cdot \varepsilon_{eff}} . \qquad (1)$$

In accordance with (1), where ε_{eff} is the effective permittivity, TM surface waves can occur on surfaces with a positive (i.e. inductive) reactance only, and thus, ε_{eff} must be positive too. For TE waves, $E_x = E_z = H_y = 0$ and the surface impedance can be derived [1], [8]

$$Z_s(TE) = -\frac{E_y}{H_z} = -\frac{j \cdot \omega \cdot \mu_{eff}}{\alpha} . \qquad (2)$$

Taking (2) into account, where μ_{eff} is the effective permeability, TE waves require the negative (i.e. capacitive) surface impedance, and thus, μ_{eff} must be positive, too.

A typical dispersion relation of TM and TE surface waves on a metal-backed dielectric slab is depicted in Fig. 3. Obviously, the surface guides TM wave from zero frequency (the surface impedance is inductive). At the frequency for which the dielectric slab thickness equals approximately one-quarter wavelength, the surface impedance becomes capacitive and the first TE wave occurs. However, the TM is still propagating: the wave simply adjusts its position toward the ground plane and the apparent surface impedance remains inductive [1], [8]. This fact is illustrated in Fig. 4, where the normalized magnetic field intensity of surface waves inside and above a metal-backed slab (thickness $h = 1.575$ mm and relative permittivity $\varepsilon = 6.15$) for different frequencies is shown. In consequence, exceeding cutoff frequency of the first TE mode, a surface-wave free dielectric slab can be achieved only by simultaneous suppression of both TM and TE polarized waves.

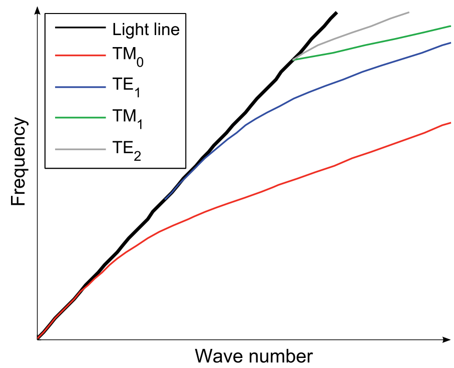

Fig. 3. Surface wave dispersion diagram of a metal-backed dielectric slab.

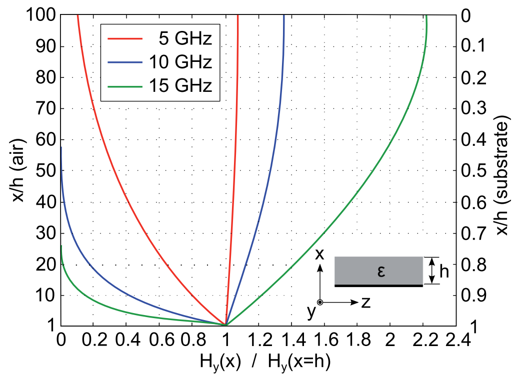

Fig. 4. Normalized magnetic field intensity of TM surface wave inside and above of a metal-backed dielectric slab ($h = 1.575$ mm, $\varepsilon = 6.15$).

Now, how to create a media with negative permittivity and/or permeability? Let us investigate the equivalent circuit representation (L-C network) of a metallo-dielectric EBG unit cell (Fig. 5). If the size of the unit cell (i.e. period of the structure *D*) is considerably smaller than the wavelength λ, the effective permittivity ε_{eff} and effective permeability μ_{eff} of the periodic media can be expressed using the series impedance *Z* and shunt admittance *Y* as [9]

$$\varepsilon_{eff} \cdot \varepsilon_0 = \frac{Y}{j \cdot \omega \cdot D} , \qquad (3)$$

and

$$\mu_{eff} \cdot \mu_0 = \frac{Z}{j \cdot \omega \cdot D} . \qquad (4)$$

In (3) and (4) ε_0 and μ_0 are the permittivity and permeability of free space, respectively. According to selection of L and C elements as the series and shunt components of the unit cell, four types of materials with different properties (positive/negative permittivity/permeability) can be created as listed in Tab. 1.

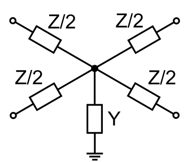

Fig. 5. Equivalent network model of a metallo-dielectric EBG.

ε_{eff}	μ_{eff}	Series L	Series C	Shunt L	Shunt C
+	+	Yes	No	No	Yes
±	+	Yes	No	Yes	Yes
+	±	Yes	Yes	No	Yes
±	±	Yes	Yes	Yes	Yes

Tab. 1. Four categories of metallo-dielectric EBGs.

Considering that the essential difference between mushroom and planar EBGs (Fig. 1) is the presence or absence of shorting vias which represent a shunt inductance in the equivalent network model, the following conclusion can be made: the mushroom EBG can suppress surface waves of both polarization (both permittivity and permeability can be negative), whereas the planar one can suppress TE waves only (permeability can be negative). However, even the mushroom EBG cannot suppress TM and TE surface waves at the same time – a medium with negative permittivity and permeability supports so-called backward-wave propagation [8], [10].

Based on the above stated, surface waves can be successfully suppressed by EBGs, if the following rules are kept:

- the antenna (exciting surface waves of both polarization) works under the first substrate TE surface wave cutoff frequency (i.e. the slab guides TM_0 mode only),
- a mushroom-type EBG is used.

If these conditions are not satisfied, the suppression of surface waves is impossible and there is only a minor (if any) improvement in radiation properties of an antenna surrounded by EBG cells. For example, the well-known uniplanar compact electromagnetic band-gap (UC-EBG) structure will never work in combination with an antenna that excites both TM and TE surface waves, because of the absence of vias. This fact can be clearly recognized e.g. in [11], [12].

For the sake of clarity, it is necessary to emphasize, that the above described equivalent network representation of metallo-dielectric EBGs and its resonant behavior, which leads to negative permittivity/permeability of the periodic medium, is valid only if the period of the structure is significantly smaller than the wavelength. When the period becomes comparable to the wavelength, typically $D \approx n(\lambda/2)$, n = 1, 2, 3..., periodic structures generate a series of stop bands. However, this phenomenon is then not related to the described unit cell resonance effect, but to Bragg's diffraction condition.

2.2 Numerical Modeling of EBGs

Let us consider a plane wave impinging on a periodic surface. For surface waves, the angle of incidence is equal to 90° (parallel with the surface). For this value, the wave propagation on a periodic structure cannot be investigated using the plane wave response [13]. The exact position of pass bands and band gaps in the frequency spectrum can be obtained only by the dispersion relation of surface waves (i.e. calculating the resonant frequencies of eigenmodes) along the contour of the irreducible Brillouin zone.

For correct EBG design, it is essential to distinguish between reflection- and dispersion response of a structure. As described in many papers, the frequency of zero reflection phase (usually calculated for normal wave incidence) does not necessarily lie inside the surface wave band gap. These two properties of EBGs crucially depend on parameters of the dielectric substrate (thickness and permittivity) and drift with variation of them [14], [15], [16].

Analysis of electromagnetic band gap structures is based on the Bloch-Floquet theorem which describes the wave propagation in infinite media consisting of periodic repetition of a unit cell. The theorem states, the properties of wave propagation in a periodic media can be fully described considering only one unit cell and applying periodic boundary conditions at its edges [17].

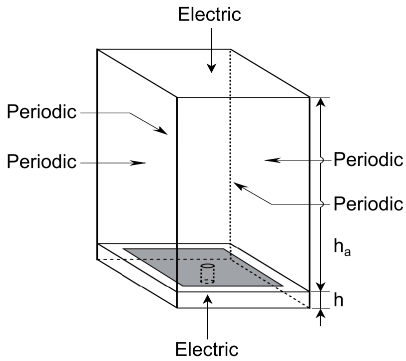

Fig. 6. Numerical model of a mushroom-type EBG unit cell in CST MWS for dispersion diagram calculation.

Nowadays, many commercial softwares are able to calculate the dispersion relation of a periodic structure using the eigenmode solver of the tool. However, the proper unit cell setup, thus, the correct surface wave diagram calculation, is another crucial point in the design of EBGs. The eigenmode solver of some tools (e.g. CST Microwave Studio, CST MWS) does not support open boundaries. In this case, the boundary condition of side walls of the unit cell can be considered periodic, but the boundaries at the top and the bottom of the model should be defined as electric conductor, see Fig. 6. The key parameter in the computer model is then the height of the air column h_a placed above the dielectric substrate to emulate the free space over the structure. Considering that surface waves are mainly concentrated inside the substrate and at the substrate/air interface, a relatively small height of the air column could be sufficient. Based on numerous computer simulations and by comparing the obtained results with analytical and experimental considerations, the correct choice of approximately ten times the substrate thickness was established, $h_a \approx 10 \cdot h$.

3. Experiments

3.1 Design of an EBG

To design electromagnetic band gap structures, numerous approximate and analytical methods were worked out [8], [18]. Nevertheless, only full-wave techniques offer an exact approach. Moreover, due to complex behavior of EBGs, stochastic methods can be successfully exploited. A combination of a full-wave numerical tool (CST MWS) with a global optimization algorithm (particle swarm optimization, PSO) was introduced in [19]. The developed technique is based on full-wave characterization of EBGs and optimization of parameters of the unit cell to fulfill the requirements. The approach is versatile and robust, applicable not only for final tuning, but also for rough initial design.

Using the CST MWS – PSO combination, a mushroom EBG was designed with surface-wave band gap at $f = 10$ GHz. The structure is realized on Arlon AD600 with thickness $h = 1.575$ mm and relative permittivity $\varepsilon = 6.15$. At the working frequency the substrate guides only the basic TM_0 surface mode (the TE_1 mode begins to propagate at $f = 21$ GHz). Optimized parameters of the unit cell are: $D = 2.22$ mm, $P = 2.04$ mm and $d = 0.40$ mm.

A board consisting 100 x 100 unit cells was fabricated and measured. The experimental setup is depicted in Fig. 7 and it was inspired by the one presented in [20].

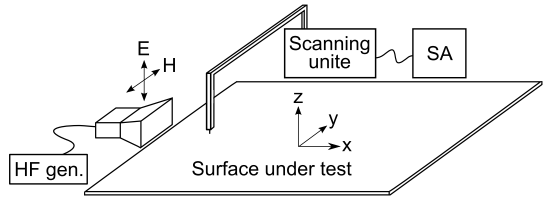

Fig. 7. Experimental setup for TM surface wave propagation measurement.

The TM surface wave propagation above the fabricated EBG and a conventional metal-backed slab made from the same dielectrics as the EBG was investigated. A small probe recording the electric field strength over the test board was used and surface-wave maps in horizontal and vertical cuts were created (the resolution is 0.25 mm in all directions). Fig. 8 shows surface wave propagation in a vertical cut over the two surfaces under investigation. The frequency was chosen $f = 10$ GHz, where the designed EBG has its band gap and strongly attenuates the propagation of TM waves. This fact is also confirmed in Fig. 9 where the TM wave attenuation in dependence on number of unit cells is shown (the field strength was recorded 1 mm above the surface). Apparently, the field intensity decreases rapidly for the first five unit cells; the impact of the rest of cells is almost negligible. Based on this fact, the effect of different number of EBG unit cells on planar antenna performance is examined in the next chapter. The main goal is to establish the basic design rules for sufficient surface waves suppression and to keep the dimensions of the antennas as small as possible.

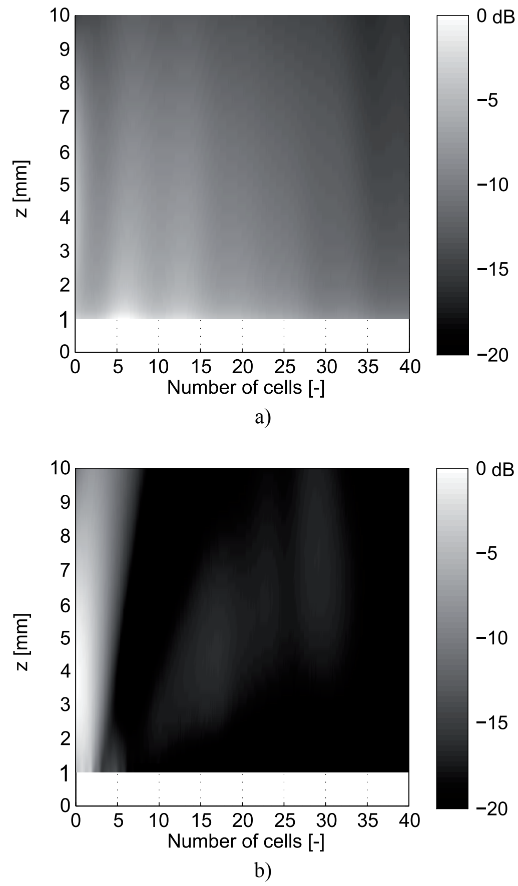

Fig. 8. Measured TM surface wave propagation at $f = 10$ GHz, x-z cut: (a) conventional metal-backed dielectric substrate, (b) EBG board. Normalized electric field intensity is shown.

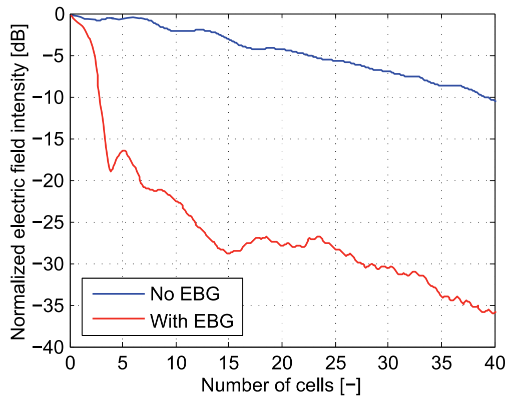

Fig. 9. Measured TM surface wave attenuation at $f = 10$ GHz along the x-axis, 1 mm over the surface.

3.2 EBG Planar Antennas

Using the mushroom structure introduced in the previous section, six coaxial probe fed planar antennas were designed, fabricated and measured at $f = 10$ GHz. The antennas were realized in three dimensions and two variants: without EBG and with EBG. For schematic view see

Fig. 10. Parameters of the antenna patch are: $A = 4.80$ mm, $B = 4.30$ mm, $C = 0.80$ mm (antennas without EBG) and $A = 5.30$ mm, $B = 4.50$ mm, $C = 1.10$ mm (antennas with EBG). The space S between the patch and the surrounding EBG is crucial in terms of impedance matching and radiation properties (shape of radiation pattern and gain) of an antenna: if S is too small, the coupling between the radiating patch and the EBG cells is too large – the antenna cannot be tuned; on the other hand, by increasing S, the effect of the EBG on antenna radiation properties decreases rapidly. This phenomenon is partially described in the literature, e.g. [21], but there is no particular recommendation for the correct choice of S. Considering a plane wave impinging on the designed mushroom surface at angle near to 90° (almost surface wave), the reflection phase response of the structure approximately 0° is obtained. The interference between the direct waves radiated by the patch and the waves reflected from the EBG is then constructive if the gap between the patch and the EBG is approximately half of the wavelength, $S \approx \lambda/2$, where λ can be estimated using the simple equation

$$\lambda = \frac{c}{f \cdot \sqrt{\frac{\varepsilon + 1}{2}}}. \tag{5}$$

In (5), c is the light velocity in free space, f is the frequency and ε is the relative permittivity of the dielectrics. In our case $\lambda \approx 16$ mm, thus $S \approx 8$ mm. Computer simulations have shown, the EBG antennas can be matched if $S \geq 3D$, i.e. $S \geq 6.66$ mm. Then, the overall size of the antennas can be determined as

$$L = 2 \cdot S + (2 \cdot n - 1) \cdot D = (5 + 2 \cdot n) \cdot D \tag{6}$$

where n is the number of EBG columns surrounding the antenna patch. For $n = 3, 6$ and 9: $L = 24.42$ mm (antenna #1), $L = 37.74$ mm (antenna #2) and $L = 51.06$ mm (antenna #3), respectively.

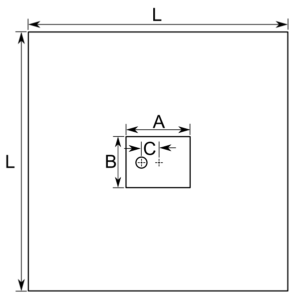

a)

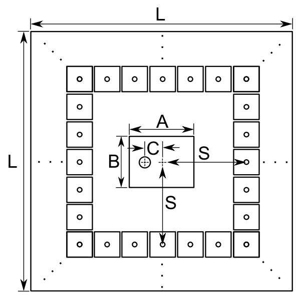

b)

Fig. 10. Schematic of coaxial probe fed planar antenna without EBG (a), with EBG (b). Top (*x-y*) view.

The measured reflection coefficient is shown in Fig. 11. Obviously, coupling between the antenna patch and the EBG is significant and produces parasitic resonances at the lower limit of the band gap (around $f = 9$ GHz). However, at the working frequency $f = 10$ GHz all the antennas are matched and the reflection coefficient is lower than –10 dB. Ripples on S_{11} curves are caused by imperfect calibration due to the use of 2.4 mm calibration set and measurement on 3.5 mm connector.

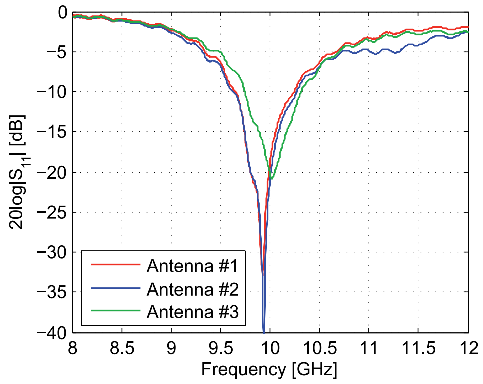

a)

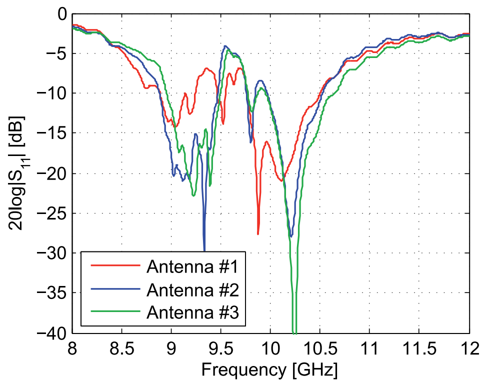

b)

Fig. 11. Measured reflection coefficient of the antennas: without EBG (a), with EBG (b).

Next, the electric field distribution 1 mm above the antennas was measured using the scanning device. As seen in Fig. 12 – Fig. 14, where the dashed line denotes the boundaries of the slab, the field strength rapidly decreases from the centre of the structure and just a small amount of energy, distributed by surface waves, reaches the boundary of the dielectric substrate if the EBG is used. This effect is apparent even for 3 columns of EBG unit cells surrounding the antenna patch.

Also radiation properties of the antennas were investigated and measured co-polar and cross-polar directivity patterns are shown in Fig. 15 – Fig. 17. For easier comparison between the antennas, the most relevant parameters are summarized in Tab. 2. In this table, the front-to-back ratio (FBR) is defined as the difference between the maximum energy emitted in the forward direction between ±30° versus the maximum energy emitted in the backward direction between ±150°. The cross-polarization level (XPL) is calculated for the forward direction between ±30°. The gain improvement (ΔG) is assumed as the difference between the maximum power radiated at 0° by the antenna without EBG versus the antenna with EBG. Efficiency η of the antennas was computed using CST MWS.

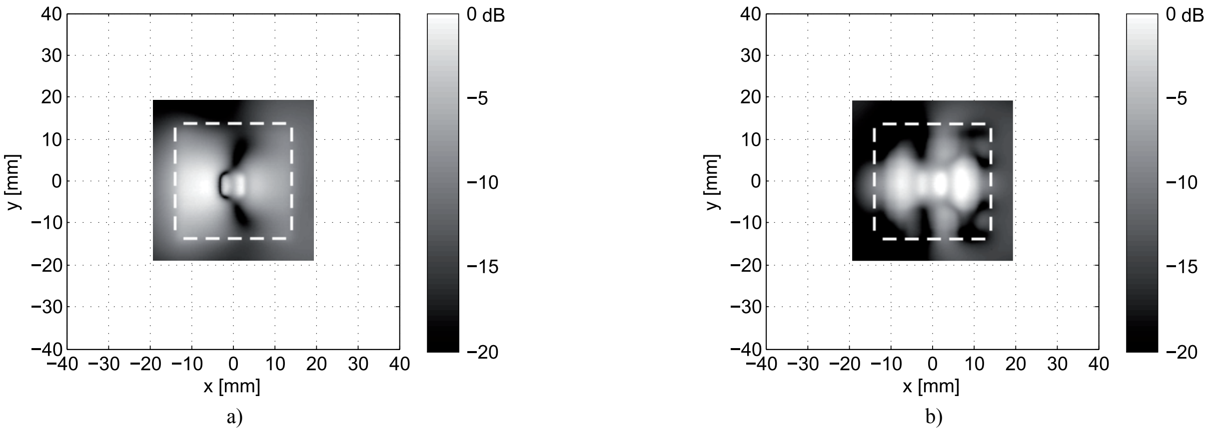

Fig. 12. Normalized electric field distribution over the antenna #1: without EBG (a), with EBG (b).

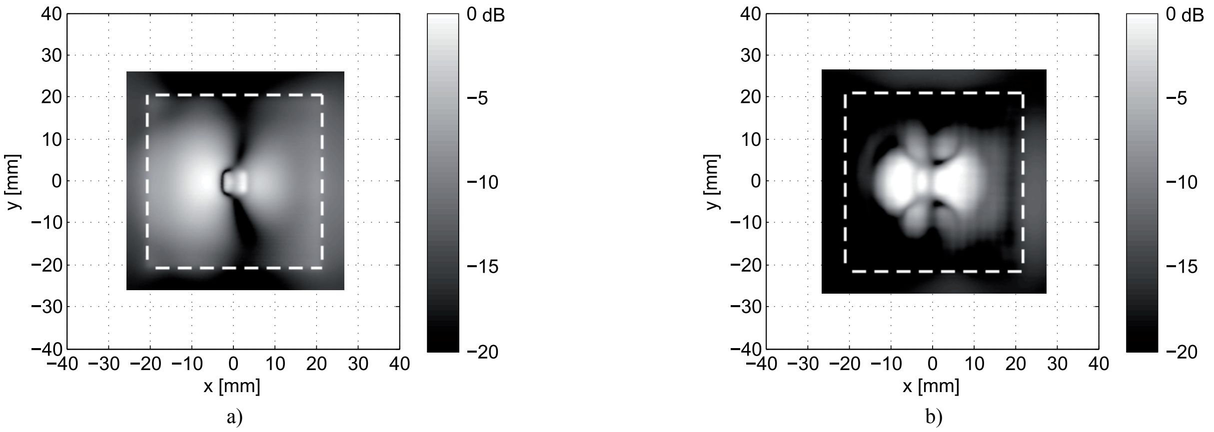

Fig. 13. Normalized electric field distribution over the antenna #2: without EBG (a), with EBG (b).

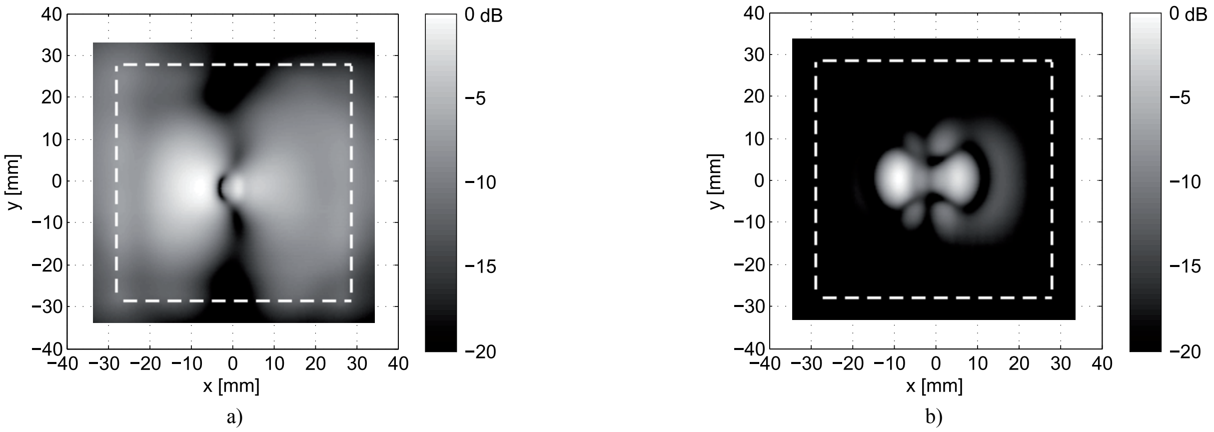

Fig. 14. Normalized electric field distribution over the antenna #3: without EBG (a), with EBG (b).

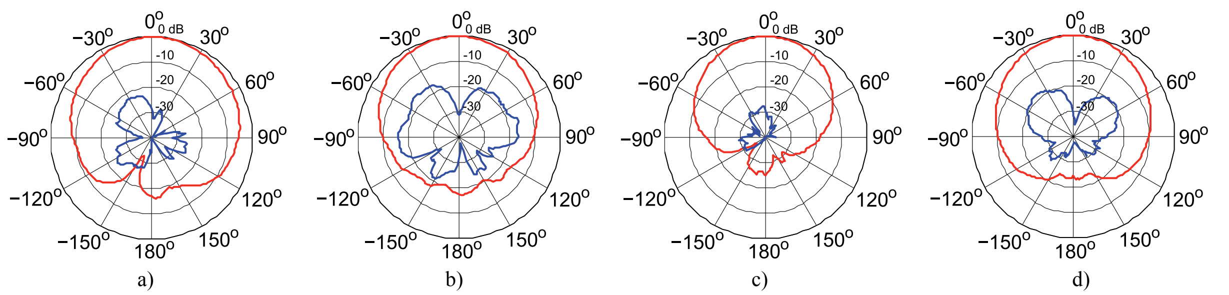

Fig. 15. Radiation pattern of the antenna #1: without EBG, E-field (a), without EBG, H-field (b), with EBG, E-field (c), with EBG, H-field (d). Red color: co-polarization, blue color: cross-polarization.

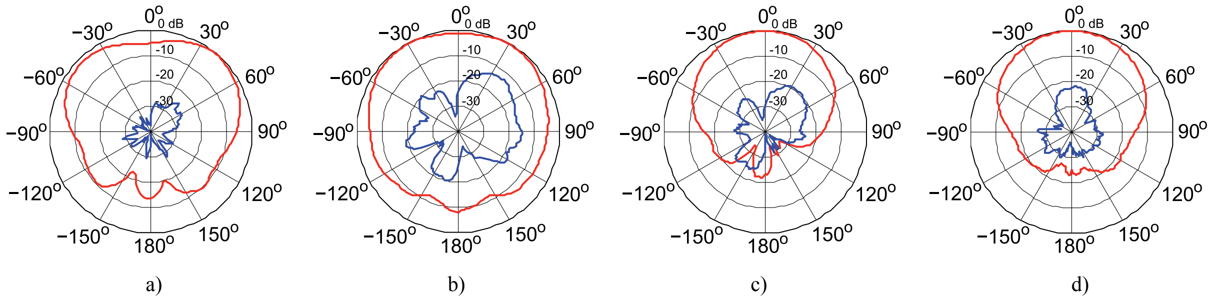

Fig. 16. Radiation pattern of the antenna #2: without EBG, E-field (a), without EBG, H-field (b), with EBG, E-field (c), with EBG, H-field (d). Red color: co-polarization, blue color: cross-polarization.

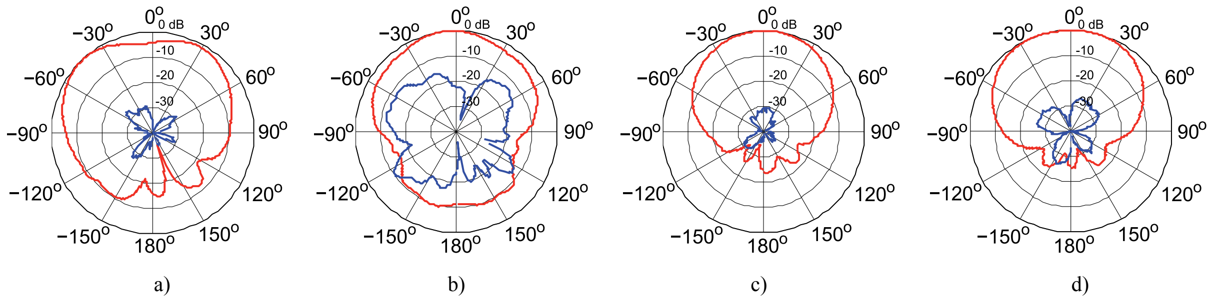

Fig. 17. Radiation pattern of the antenna #3: without EBG, E-field (a), without EBG, H-field (b), with EBG, E-field (c), with EBG, H-field (d). Red color: co-polarization, blue color: cross-polarization.

	Antenna #1				Antenna #2				Antenna #3			
	W/O EBG		With EBG		W/O EBG		With EBG		W/O EBG		With EBG	
Plane	E	H	E	H	E	H	E	H	E	H	E	H
FBR [dB]	16.1	16.6	23.5	21.6	11.6	7.7	20.9	21.1	10.2	9.3	23.3	24.7
XPL [dB]	-20.8	-16.3	-23.2	-18.9	-25.2	-13.7	-18.0	-20.1	-28.5	-15.6	-30.3	-26.3
ΔG [dB]	–		2.1		–		5.3		–		5.4	
η [%]	95.9		99.2		96.6		99.5		96.9		99.6	

Tab. 2. Radiation properties of the fabricated antennas without and with EBG.

The general conclusions are the following: The antennas with EBG in comparison with their counterparts without EBG have smooth and almost symmetric radiation patterns, significantly better front-to-back ratio and lower cross-polarization level. Performance of EBG antennas with different number of unit cells, vary in a relatively small way: the major difference is apparent in the antenna gain, which is also the consequence of smaller or larger aperture size. The benefit of EBG antennas in comparison with conventional ones is unambiguous. The number of unit cells to be chosen always depends on requirements and maximum allowed dimensions.

4. Conclusions

More than two decades after they have been introduced, electromagnetic band gap structures still play important role in microwave and antenna engineering. Following contemporary trends, microwave devices and antennas are moving to millimeter-wave and submillimeter-wave frequency bands. Besides numerous advantages of the new radio spectra, engineers are forced to challenge new difficulties. For example, antenna designers are facing to significant losses appearing in planar antennas, especially in antenna arrays, resulting in decreased antenna gain and thus, larger structure. Moreover, most of the energy emitted by an antenna is formed into surface waves and leads to distorted radiation pattern and very poor front-to back ratio. EBGs represent a promising way to overcome some of these problems and to make possible to design e.g. high-gain, compact antenna arrays with the desired radiation properties in a relatively simple way. The key to the success is the correct implementation of EBGs. Unfortunately, there are some common mistakes and misunderstandings related to theory, design and practical application of electromagnetic band gap surfaces in antennas technology. Our aim was to give a clear and simple explanation about the basics of metallo-dielectric EBGs and to demonstrate their practical exploitation on practical examples. The most original part of the work is the investigation of different number of EBG unit cells on planar antenna radiation properties. The presented results could be helpful for designers to achieve the desired antenna performance for minimum structure dimensions.

Acknowledgements

The research leading to these results has received funding from the European Community's Seventh Framework Programme (FP7/2007-2013) under grant agreement no. 230126. The research described in this contribution was performed in the laboratories supported by the SIX project; the registration number CZ.1.05/2.1.00/03.0072, the operational program Research and Development for Innovation.

References

[1] COLLIN, R. *Field Theory of Guided Waves*. 2nd edition. IEEE Press, New York, 1991.

[2] BROWN, E. R., PARKER, C. D., YABLONOVITCH, E. Radiation properties of a planar antenna on a photonic-crystal substrate. *J. Opt. Soc. Am. B*, 1993, vol. 10, no. 2, p. 404-407.

[3] YOOK, J.-G., KATEHI, L. Micromachined microstrip patch antenna with controlled mutual coupling and surface waves. *IEEE Transactions on Antennas and Propagation*, 2001, vol. 49, no. 9, p. 1282-1289.

[4] ALEXOPOULOS, N. G., JACKSON, D. R. Fundamental superstrate (cover) effects on printed circuit antennas. *IEEE Transactions on Antennas and Propagation*, 1984, vol. 32, no. 8, p. 807-816.

[5] JACKSON, D. R., WILLIAMS, J. T., BHATTACHARYYA, R. K., SMITH, R. L., BUCHHEIT, S. J., LONG, S. A. Microstrip patch designs that do not excite surface waves. *IEEE Transactions on Antennas and Propagation*, 1993, vol. 41, no. 8, p. 1026-1037.

[6] YABLONOVITCH, E. Inhibited spontaneous emission in solid state physics and electronics. *Physical Review Letters*, 1987, vol. 58, p. 2059-2062.

[7] JOHN, S. Strong localization of photons in certain disordered dielectric super lattices. *Physical Review Letters*, 1987, vol. 58, p. 2486-2489.

[8] SIEVENPIPER, D. F. High-impedance electromagnetic surfaces. *Ph.D. Thesis*, Los Angeles (CA, USA), 1999.

[9] SANADA, A. Planar single- and double negative metamaterial implementations and applications. *URSI*, 2005. Available online at: http://www.ursi.org/Proceedings/ProcGA05/pdf/D02.3%2801244%29.pdf

[10] STRATTON, J. *Electromagnetic Theory*. Wiley, 1941.

[11] COCCIOLI, R., YANG, F.-R., MA, K.-P., ITOH, T. Aperture-coupled patch antenna on UC-PBG substrate. *IEEE Transactions on Microwave Theory and Techniques*, 1999, vol. 47, no. 11, p. 2123-2130.

[12] LAMMINEN, A. E. I., VIMPARI, A. R., SAILY, J., UC-EBG on LTCC for 60-GHz frequency band antenna applications. *IEEE Transactions on Antennas and Propagation*, 2009, vol. 57, no. 10, p. 2904-2912.

[13] GOUSETTIS, G., FRESEDIS, A. P., VARDAXOGLOU, Y. C. Tailoring the AMC and EBG characteristics of periodic metallic arrays printed on grounded dielectric substrate. *IEEE Transactions on Antennas and Propagation*, vol. 54, no.1, 2006, p. 82-89.

[14] CLAVIJO, S., DIAZ, R. E., McKINZIE, W. E. Design methodology for Sievenpiper high impedance surfaces: an artificial magnetic conductor for positive gain electrically small antennas. *IEEE Transactions on Antennas and Propagation*, 2003, vol. 51, no. 10, p. 2678-2690.

[15] AMINIAN, A., YANG, F., RAHMAT-SAMII, Y. In-phase reflection and EM wave suppression characteristics of electromagnetic bandgap ground planes. In *Proc. IEEE AP-S Int. Symp.*, 2003, vol. 4, p. 430-433.

[16] LI, L., CHEN, Q., YUAN, Q., LIANG, C., SAWAYA, K. Surface-wave suppression bandgap and plane-wave reflection phase band of mushroomlike photonic bandgap structures. *J. Appl. Phys.*, 2008, vol. 103, no. 2, p. 023513-023513-10.

[17] ENOCH, S., TAYEB, G., MAYSTRE, D. Dispersion diagrams of Bloch modes applied to the design of directive sources. *Progress in Electromagnetics Research series*, 2003, vol. 41, p.61-81.

[18] TRETYAKOV, S. *Analytical Modeling in Applied Electromagnetics*. Artech House, 2003.

[19] KOVACS, P., RAIDA, Z. Design and optimization of high-impedance surfaces. *International Journal of RF and Microwave Computer-Aided Engineering*, accepted for publication.

[20] MATSUGATANI, K., TANAKA, M., FUKUI, S., KIM, W. H., KIM, M. Surface wave distribution over Electromagnetic Bandgap (EBG) and EBG reflective shield for patch antenna. *IEICE Trans. Electron.*, 2005, vol. E88-C, no. 12, p. 2341-2349.

[21] ILUZ, Z., SHAVIT, R., BAUER, R. Microstrip antenna phased array with electromagnetic bandgap substrate. *IEEE Transactions on Antennas and Propagation*, 2004, vol. 52, no. 6, p. 1446-1453.

About Authors ...

Peter KOVÁCS was born in Slovakia. He received the Ph.D. degree from the Faculty of Electrical Engineering and Communication (FEEC), Brno University of Technology (BUT), Czech Republic, in 2011. Currently, he is with the Dept. of Radio Electronics FEEC BUT.

Tomáš URBANEC was born in Třinec, Czech Republic. He received his M.Sc. from Brno University of Technology in 2000 and his Ph.D. in 2007. Since 2007, he has been an assistant at the Dept. of Radio Electronics, BUT. He is interested in microwave measurement and design.